J Therm Anal Calorim (2012) 107:1353–1361
DOI 10.1007/s10973-011-1668-5

Well surveillance using multivariate thermal measurements

Kobra Pourabdollah · Bahram Mokhtari

Received: 25 February 2011 / Accepted: 13 May 2011 / Published online: 28 May 2011

Abstract Traditional methods to measure and survey the productivity of oil wells mainly consisted of using test-separator units with expensive instrumental, mechanical, electrical, piping, and safety devices along with technical and protective inspections, repair and operation services, facilities, and infrastructures. Their inherent limitations are time and cost consuming, uncertainty of well isolation in test separator, and need to close the co-line wells, which are diminished using multivariate thermal well testing. In this study, an alternative method is presented using multivariate regression on thermal analysis data. The objective of this study, which covered three distinctive major fields of statistics, thermal analysis, and well testing, is predicting the accurate productivity of oil wells using a single sample point at the blend oil pipeline. This method is based in performing multivariate regression of thermogravimetric data obtained from the samples of Iranian offshore oil wells. The results revealed that the used model appropriate for crude oil blends, which thermal traces significantly differ from each other. The calculated error function corrected the blend equation by considering the eutectic points and catalytic pyrolysis in lower and higher temperatures, respectively. The model predicted the accurate productivity of oil wells in real samples of blend oil pipeline.

Keywords Multivariate regression · Thermal analysis · Well test

K. Pourabdollah (✉) · B. Mokhtari
Department of Chemical Engineering, Shahreza Branch, Islamic Azad University, Shahreza, Iran
e-mail: pourabdollah@iaush.ac.ir

Introduction

Well performance testing is widely used to determine the productivity of oil wells. Historically, the oil industry has relied on traditional methods for individual well flow monitoring. The first and the widespread technique of well testing is multi-plot method, in which the production rate of candidate well is plotted versus a variable parameter to optimize the variable situation and to achieve the maximum productivity. This provides periodic well test information using test-separators and sometimes supplemented with real time temperature and pressure data gathered from the individual wells between tests (see Fig. 1).

The empirical relationships used to estimate rate between valid tests are often hampered by uncertainties and errors associated with data limitations and varying flow conditions. In addition, restricted access to the test-separator often imposes constraints on when this information can be gathered. Moreover, as the heavy oil has a density similar to that of produced water, the use of test-separators is not practical. The second technique of well testing is well logging method, in which the logging tools provide flow information as a function of well depth and intermittently in time. However, the logs are complicated, especially those designed for deviations beyond 45° from vertical, where sophisticated hardware with sensor arrays must be combined with empirical slip models to cope with unsteady and non-uniform flows. Both conventional well tests include a deliberate disturbance to the production to determine the dynamic characteristics of a well. Moreover, these traditional routine well testing methods simply provide a series of snap-shots of a well's performance, which may or may not reflect the production during the intervening period. Furthermore, since those methods are normally shared among a number of wells, the actual

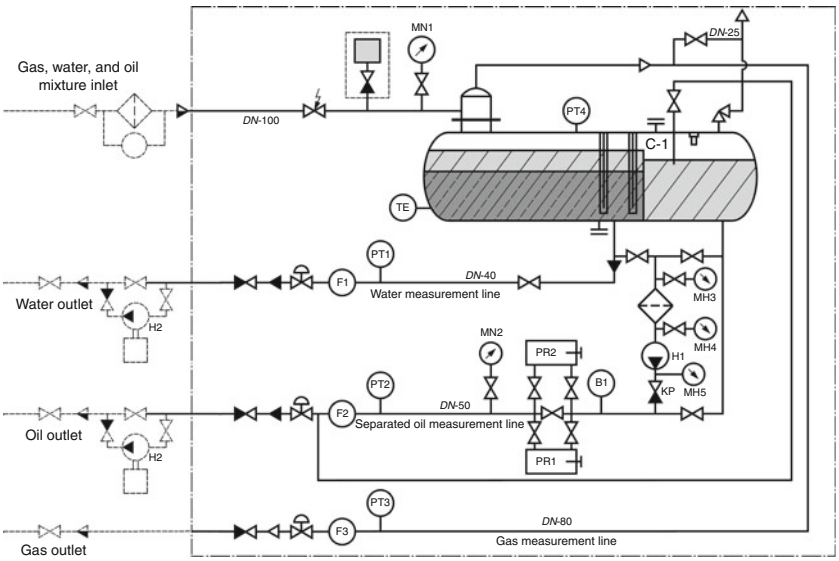

Fig. 1 Schematic diagram of a test-separator unit

performance of a well is only measured periodically or on demand. Typically about 0.1–2.0% of the well production is measured by these well testing methods. Thus, the surveillance of individual oil wells is a discontinuous periodic process. This is not optimal, as many well problems are not determined until a well is re-tested.

These conventional flow-monitoring methodologies are premised on the concept that oil production systems were largely steady state and these snap shots in time were adequate to manage the production. Besides, well test conditions of isolated wells may be very different from actual operating conditions with the parallel wells. However, in many oil fields, the well performance and the plant-operating conditions can change rapidly and there is value in more regular and closer well production monitoring. In addition, when an oil field enters a production decline, it requires a higher frequency of data gathering and higher level of attention. Gathering real time data from oil wells and related facilities has not been an issue, but validating the gathered data, relating them to the production rates of individual wells in a coherent manner, and then taking prompt action is a challenge.

Historical review

In the early 1980's, the multiphase flowmeters were developed to be used in well testing. When the gas oil ratio (GOR) is not too high and there is a room at the wellhead surface, the surface multiphase flowmeters can be used, but they have proved problematic owing to the high volume of associated gas that evolves from the oil stream in pipe or well, complicating the determination of oil or water volumes. On platforms servicing many wells, there may not be enough room or suitable space to install a multiphase meter on each well, thus preventing continuous flow rate and cut measurements on each of the wells. As found in the test-separator method, this introduces the same type of uncertainty owing to varying flow conditions. Recently, downhole multiphase flowmeters have relied on a venturi device combined with a pressure gauge. The combination of differential pressure across the venturi and density provides total mass flow rate. However, there are some difficulties with these flowmeters. First, in multiphase wells (such as gas lifted wells) they are not applicable. Second, in horizontal or high-angle wells or where, there are multiple pay zones, there is insufficient hydrostatic head for a practical density reading. Third, the simple measurement of hydrostatic density ignores the slip effect between the phases.

Measuring the three-phase fluids, such as crude oil in the wells and the pipelines is the subject of many researches [1]. Preparation of blown venturi flowmeters [2], estimating the bubble point in petroleum fluids flow line [3], and using dielectric spectroscopy for characterization of annular fluids pumped from an oil layer [4] show some advances in this field. Tan and Dong [5] measured the oil–water two-phase flow rate by a V-cone meter. Wang et al. [6] measured the in situ multiphase flow of oil, gas, and water in a well fluid using a prompt gamma-ray neutron activation analysis (PGNAA) and an on-line oil flowmeter based upon the measurement of dielectric properties was also reported [7].

Multivariate thermal model

It is well recognized that thermogravimetry (TG) and differential scanning calorimetry (DSC) are rapid tools, which

have been used in a wide variety of areas related to crude oil analysis [8–13], coal reactivity, heat effect associated with coal pyrolysis, biomass and mineral oils [14], combustion, and kinetics [15]. Thermal analysis enables physical and chemical phenomena occurring in the substance investigated during heating. Since the late 1960's and early 1970's, thermal analysis methods have been used to characterize petroleum and related products. DSC commonly used to determine crystallinity because it is rapid and more convenient than wet chemical methods that require solvents for the extraction of crystallizing waxes. Fulem et al. [16] studied the phase behavior of Maya crude oil and its nano-filtered sub fractions using DSC and constructed the composition phase diagram for Maya crude oil. Gjurova et al. [17] assessed the influence of the analytical conditions, the kind and the amount of the petroleum and petroleum products on the temperature interval of separation, the accuracy, the reproducibility and the detection limit. Shishkin [18] examined the group hydrocarbon composition of crude oils and oil heavy residues using TG and DSC. In hyphenated techniques, the multiple data is gathered during one run of experiment. These multiple data can be including the type of the volatile products as a function of the temperature, the mass loss of the sample as a function of the temperature, and the quantitative analysis of the evolved gases.

Evolved gas analysis (EGA) using hyphenated TG-Fourier transform infrared spectroscopy (TG-FTIR) was reported as a very useful tool to study the thermal decomposition of sewage sludge [19] by means of multivariate analysis techniques. With the growing popularity of coupled instruments, statistics models for manipulating two-dimensional data have been developing. The increasing memory capacity and computing power of the current computers further expedites the process. The major advantage of multivariate data is to extract more information from mountainous two-dimensional data. Pyrolysis–gas chromatography–mass spectrometry (Py–GC–MS) was used to study the thermal decomposition of Kraton 1107 copolymer. Principal component analysis (PCA) and contour variance diagram were used for performing the factor analysis. Statheropoulos et al. [20] used these results for determination of the main thermal decomposition steps of Kraton 1107 copolymer.

Smidt et al. [21] used simultaneous thermal analysis methods (TG–MS and DSC) and compared a large data pool of treated municipal solid waste originating from different treatment plants. They concluded that thermal analysis in association with multivariate statistical methods could be a reliable method to verify efficient separation of the plastic fraction, stabilization, and waste material composition. Application of hyphenated thermal-statistical methods is not limited to oil industry and there are many researches, such as the study of Miltyk et al. [22] in pharmaceutical studies. They completely discussed an example of building discriminant models against the presence of acetaminophen in tablet. They used partial least squares discriminant analysis (PLS-DA) against detection of acetaminophen in the formulations and they found a good model with root mean square error (RMS), root mean square error of cross-validation (RMSECV), and root mean square error of prediction (RMSEP) equal to 0.1068 (98.8% of explained variance), 0.148 (97.7% of explained variance), and 0.3918 (86.5% of explained variance), respectively.

This article is intended to introduce the project of author's dissertation at a high level and share some of the laboratorial experiences and findings of the first phase of its development. The proposed model, which is based upon thermal analysis in association with multivariate statistical methods, is a reliable method to verify efficient oil well surveillance. This was used for well-by-well production surveillance and it can be operational at many of production facilities worldwide, both offshore and onshore. In addition, it can help resolve hydrocarbon allocation problems through real time reconciliation, increase production through improved monitoring, allow an increase in time between reduce travel to field locations and well tests.

Thermogravimetric theoretical models

The disappearance rate of a reactant during heating process is assumed to be depended on two variables of conversion degree and temperature. The general equation of reaction rate in simple reactions is presented in Eq. 1 [23, 24]

$$\acute{\alpha} = \frac{\mathrm{d}\alpha}{\mathrm{d}t} = k(T)g(\alpha), \tag{1}$$

where $\acute{\alpha}$ is the conversion rate of reactions, α depicts the conversion degree (Eq. 2), t and T symbolize the heating time and the temperature, respectively, and $k(T)$ and $g(\alpha)$ accounts for the temperature and conversion dependence of the reaction (Eqs. 3, 4), respectively.

The conversion degree refers to the rate of sample undergoing the reaction up to a defined temperature and is determined by Eq. 2 [24]

$$\alpha = \frac{m_\mathrm{i} - m_\mathrm{t}}{m_\mathrm{i} - m_\mathrm{f}} \qquad 0 < \alpha < 1 \tag{2}$$

where m_i and m_f are the initial and final masses of the sample reacted, while m_t presents the mass of the sample at a certain time. Arrhenius equation in Eq. 3 [24] describes the temperature dependence of kinetic constant, $k(T)$

$$k(T) = A \exp\left(\frac{-E}{RT}\right), \tag{3}$$

where A is the Arrhenius constant, and E and R show the activation energy and gas constant, respectively. As Eq. 4 presents, the nth order reaction model is often used for TG analysis of crude oils.

$$g(\alpha) = (1-\alpha)^n. \tag{4}$$

In dynamic conditions, the temperature varies linearly with time with a constant heating rate (Eq. 5)

$$\beta = \frac{dT}{dt}. \tag{5}$$

Free model of Kissinger

Kissinger assumed that the reaction rate reaches to its maximum at a peak temperature in differential thermogravimetry (DTG) trace and proposed Eq. 6 [23, 25–27].

$$\ln\left(\frac{\beta}{T_p^2}\right) = \ln\left(-\frac{AR}{E}g'(\alpha_p)\right) - \frac{E}{RT_p}, \tag{6}$$

where T_p stand for peak temperature. The activation energy is calculated from the slope of the straight line. Since the peak temperatures are used in Eq. 8, one single E is given by this model.

Free model of Augis Bennett

This model is based upon the thermal theory of transformation kinetics, developed by Avrami [28]. Equation 7 depicts this model [29].

$$\ln\left(\frac{\beta}{T_p - T_o}\right) = \ln A - \frac{E}{RT_p} \tag{7}$$

T_o shows the onset temperature of DTG peak. As a result of this model, an overall single value is obtained for E.

Free model of Ozawa Flynn wall (OFW)

In this model, according to Eq. 8, the temperature values at fixed conversion degrees are measured for different heating rates [23, 30]. In a constant α, the plot of $\ln\beta$ versus $1/T$, obtained from the curves recorded at several heating rates, should give straight lines whose slopes gives E.

$$\ln\beta = \left(\ln\frac{AE}{Rg(\alpha)} - 5.331\right) - 1.052\frac{E}{RT}. \tag{8}$$

Free model of Kissinger Akahira Sunose (KAS)

This model (Eq. 9) is run like the OFW method to calculate E [23].

$$\ln\left(\frac{\beta}{T^2}\right) = \ln\frac{AR}{Eg(\alpha)} - \frac{E}{RT}. \tag{9}$$

Free model of Friedman

When combining Eqs. 1–5, the Friedman model (Eq. 10) becomes, which suggests a differential method. For a constant α, the plot of $\ln[\beta(d\alpha/dT)]$ versus $1/T$, obtained from experimental data recorded at several heating rates, should be a straight lines whose slopes allow the evaluation of activation energy.

$$\ln\left(\beta\frac{d\alpha}{dT}\right) = \ln A + \ln(g(\alpha)) - \frac{E}{RT}. \tag{10}$$

Free model of Freeman Carroll

All the kinetic parameters in this model (Eq. 11) are evaluated by a single TA curve [23].

$$\frac{\Delta\ln\acute{\alpha}}{\Delta\ln(1-\alpha)} = -\frac{E}{R}\frac{\Delta(1/T)}{\Delta\ln(1-\alpha)} + n. \tag{11}$$

Fitting model of Coats Redfern

This is the most popular fitting method (Eq. 12) for kinetic analysis of TG [31].

$$\begin{cases} \ln\left(\dfrac{-\ln(1-\alpha)}{T^2}\right) = \ln\left(\dfrac{AR}{\beta E}\left(1-\dfrac{2RT}{E}\right)\right) - \dfrac{E}{RT} & n=1 \\ \ln\left(\dfrac{1-(1-\alpha)^{1-n}}{T^2(1-n)}\right) = \ln\left(\dfrac{AR}{\beta E}\left(1-\dfrac{2RT}{E}\right)\right) - \dfrac{E}{RT} & n\neq 1 \end{cases}. \tag{12}$$

Fitting model of Arrhenius

Arrhenius in Eq. 13 assumed that the rate of sample mass loss depends on the mass of the sample remaining, the rate constant, and the temperature.

$$\mathrm{Log}\left(\frac{dw/dt}{w}\right) = \log A - \frac{E}{2.303RT}, \tag{13}$$

where w is the mass of sample remaining. When the curve is plotted, there appears to be regions of marked linearity. The slope of such a linear portion is proportional to E, and the intercept to A.

Fitting model of maximum point

Decomposition rate reaches to a maximum value at the peak of DTG curve. According to Eqs. 14 and 15, this peak point at a single heating rate is used to evaluate the kinetic parameters such as A and E. The main disadvantage of this model is that only a single point in the thermogravimetric curve is used.

$$A = \left(\frac{\beta E}{RT_m^2}\right)\exp\left(\frac{E}{RT_m}\right) \tag{14}$$

$$E = \frac{RT_m^2}{\gamma_m}\left(-\frac{dw}{dT}\right)_m, \quad (15)$$

where T_m presents the absolute temperature at the maximum rate of mass loss and γ_m is the sample fraction, remaining at the maximum rate of mass loss.

Fitting model of Ingraham marrier

This model (Eq. 16) determines heterogeneous reactions exhibiting linear kinetics.

$$\mathrm{Log}\left(\frac{dw}{dT}\right) = \log A - \log\beta - \log T - \frac{E}{2.303RT}. \quad (16)$$

Fitting model of Horowitz Metzger

This model is fitted for first order kinetics ($n = 1$) and is depicted as Eq. 17. By plotting the logarithmic term against θ, the activation energy is obtained [32].

$$\ln(-\ln(1-\alpha)) = \left(\frac{E\theta}{RT_p^2}\right), \quad (17)$$

where $\theta = T - T_p$.

Experimental method

Materials and samples

The oil samples were collected from one of the Iranian offshore fields and their physical properties and chemical characteristics (as the blend of individual wells) are presented in Tables 1, 2, respectively. The studied oil field is consisted of five oil wells with different production rates. Table 3 presented the characteristics of oil wells and exported blend line.

Instrument and method

The TG and DTG experiments were performed using the LABSYS^{TM} model D/LABTG-1A thermal analyzer system. In dynamic thermal analysis tests, six samples ($\sim$9 mg) were heated from room temperature to 700 °C at 10 °C min^{-1} under nitrogen (100 mL min^{-1}) atmosphere. The calculations were performed using the Setsoft software (see Fig. 2).

Calibrations

Two types of calibration were conducted for TG analyzer, including temperature and mass calibration. The temperature was calibrated by Curie point method. Calibration for mass change was carried out by addition and removal of standard mass on the sample holder.

Result and discussions

The weighed sum method (WSM) model

The WSM, which is based upon partial least square (PLS), was introduced as the simplest approach to correlate the thermogravimetric trace of blend oil to those of its single components or individual oil wells. This approach, which is mathematically formulated as Eq. 18, assumes a linear behavior of the blend oil with respect to the mass fractions of its constituents [33]. This approach has been widely applied in science and engineering to express the pyrolysis of biomass as a sum of its major components i.e., hemicelluloses, cellulose, and lignin [34–36].

$$Y_{mix} = x_1y_1 + \ldots + x_ny_n + \varepsilon = \sum_{i=1}^{n} x_iy_i + \varepsilon \quad (18)$$

where Y_{mix} is the calculated value at the thermogravimetric trace of blend oil and y_i the measured value at a thermogravimetric trace of constituent i. n is the number of individual oils taken into account and the coefficients x_i are unknown (i.e., the mass fractions of each component i in the blend). ε depicts the error function of this model. To minimize the difference between the measured and the calculated values, the PLS method was used for the x_i in Eq. 18. The objection function of S_R is defined as Eq. 19:

Table 1 Physical properties of the blend crude oil used in the experiments

Specification	Quantity	Test method
Density/60°F	0.8092/g cm^{-3}	ASTM D-4053
Density/70°F	0.8035/g cm^{-3}	ASTM D-4054
Density/80°F	0.7989/g cm^{-3}	ASTM D-4055
Viscosity/60°F	2.2139/cp	ASTM D-445
Viscosity/70°F	1.9608/cp	ASTM D-445
Viscosity/80°F	1.7133/cp	ASTM D-445
Acidity number	0.29/mg KOH g^{-1}oil	ASTM D-664

Table 2 Chemical characteristics of the blend crude oil used in the experiments

Component	Flashed liquid/mol%	Flashed gas/mol%	Stream liquid/mol%
N_2	00.00	00.31	00.04
CO_2	00.00	02.78	00.35
H_2S	00.00	04.52	00.57
CH_4	00.00	30.14	03.76
C_2H_6	00.00	12.02	01.50
C_3H_8	01.18	21.90	03.77
i-C_4H_{10}	01.16	07.25	01.92
n-C_4H_{10}	06.49	12.40	07.23
i-C_5H_{12}	02.73	03.21	02.79
n-C_5H_{12}	03.94	02.81	03.80
C_6	08.08	01.86	07.30
C_7	09.91	00.68	08.76
C_8	10.97	00.12	09.61
C_9	10.02	00.00	08.77
C_{10}	07.71	00.00	06.75
C_{11}	04.12	00.00	03.60
C_{12+}	33.69	00.00	29.48
Total sulfur	00.85/mass%		
Asphaltene	00.32/mass%		
Wax	05.00/mass%		

Table 3 Characteristics of the individual oil wells and the exported blend pipeline

Oil well	Productivity range/BPD[a]	Water content/%	Well head pressure/bar	Well head temperature/°C	GOR[b]/SCF[c]/BBL^{-1}
Bl 2P	400–500	0	14	41	200
Bl 4P	4,200–4,400	25	30	66	266
Bl 5P	9,400–10,000	1	55	68	309
Bl 6P	7,100–7,500	23	18	67	347
Bl 12P	3,200–3,600	5	18	49	0
Export line	25,000–26,000	0	19	52	–

[a] Barrels per day

[b] Gas oil ratio

[c] Standard cubic feet per barrel

$$S_R = \sum_{N_{\text{data}}} (y_{\text{mix}} - Y_{\text{mix}})^2 = \sum_{N_{\text{data}}} \left(y_{\text{mix}} - \sum_{i=1}^{n} x_i y_i \right)^2, \quad (19)$$

where y_{mix} shows the measured value at a thermogravimetric trace of individual oils and N_{data} presents the amount of data points taken into account. The WSM is applied separately to the thermogravimetric traces. The Excel Microsoft was used for the multivariable constrained minimization. To test the WSM, synthetic mixtures containing five crude oils from each of the wells were prepared. Several synthetic blends were analyzed and one of them is discussed, which consists of five crude oil samples from five oil wells. Figure 3 illustrates the TG traces of oil samples and blend oil. These traces were normalized based upon the mass remained after 600 °C. Figure 4 depicts the related normalized TG curves.

According to Fig. 3, at the end of thermal program, 40, 40, 50, 60, and 90% of oils from *Bl 2P* to *Bl 12P* were remained without pyrolysis, respectively. This led to remain about 60% of blend oil. Figure 5 shows the DTG traces of oil samples. In this study, the maximum evaporation rates were observed at 179, 168, 195, 163, and 194 °C for oil samples of individual wells from *Bl 2P* to *Bl 12P*, respectively. The DTG peak of blend (export) oil take place at 158 °C.

According to Eq. 18, vector **x** was modeled as sum of outer products between score vectors (**a**) and loading

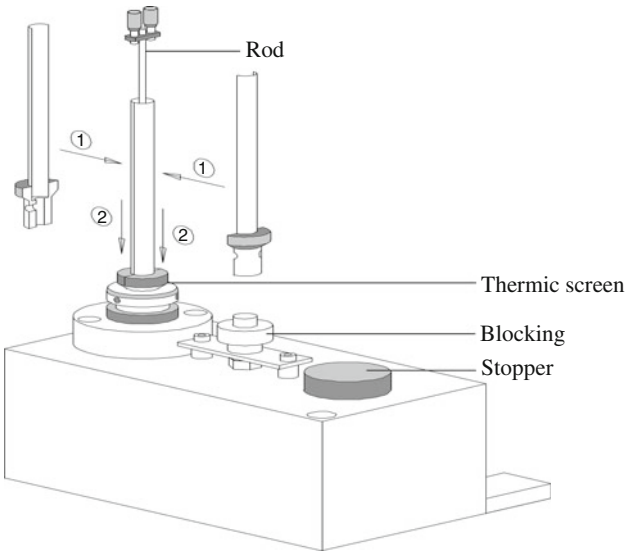

Fig. 2 Schematic diagram of the thermal analyzer apparatus

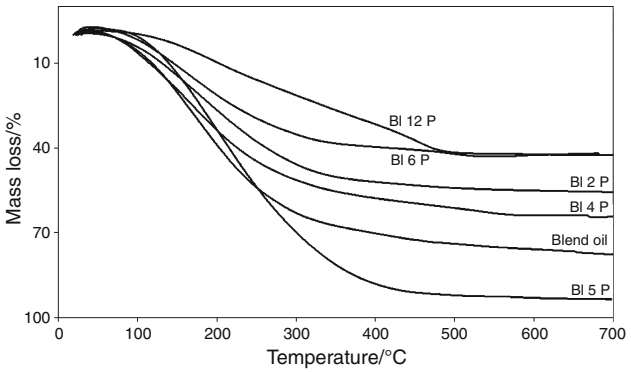

Fig. 3 The TG curves of oil samples and blend oil

vectors (**b**), where summation goes over all latent variables extracted:

$$\mathbf{x} = \sum_{i=1}^{n} \mathbf{a}_i \mathbf{b}_i^T + \varepsilon. \tag{20}$$

The thermogravimetric data have been arranged in a two-way array by taking the five samples for each of the oil samples as columns and the thermal signal intensities (570 points) as rows, obtaining an A-matrix of dimensions 571 × 5 (Fig. 6).

According to schematic of Fig. 6, the **b** vector represents the mass fractions of pure components (individual wells). This leads to calculate the proportional mass productivity of oil wells after multiplying to their density. Multiplying the resulted proportional volume productivities by blend or exported flow gives the real productivity of oil wells. The important parameter is computing the error vector (**ε**) to be added to $\mathbf{A}\mathbf{b}^T$ product. After computing the error vector, a simple classical least square technique

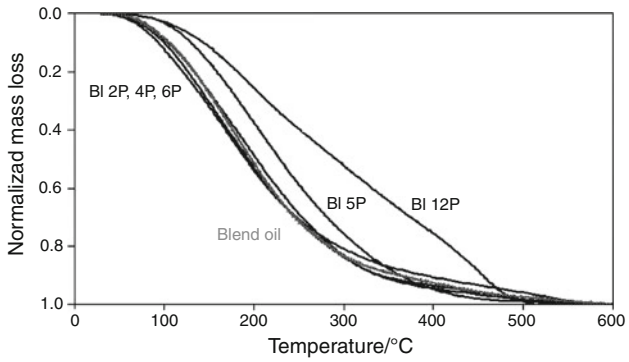

Fig. 4 Normalized TG curves of oil samples

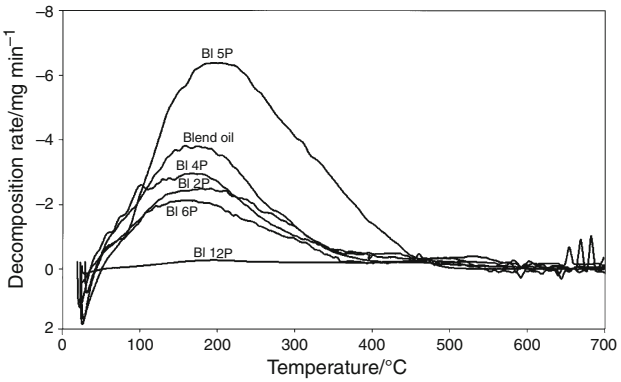

Fig. 5 The DTG curves of crude oil samples and blend

solves the equation and the **b** vector is obtained. According to Eq. 21, using Matlab software, the **b** vector was obtained for synthetic oil blends.

$$\mathbf{b} = \mathbf{A} \backslash (\mathbf{x} + \varepsilon). \tag{21}$$

Error assessment

It is possible that a thermal degradation peak found for an unknown blend oil does not correspond to a peak of an individual samples taken from each well. In the following, it is examined how sensitive the calculated blend oil is for changes in the single components trace. Using synthetic blend oils, the vector **ε** was calculated and the resulted graph is presented in Fig. 7.

According to Fig. 7, two distinct zone of evaporation eutectic (ee) and catalytic cracking (cc) shows the main sources of negative and positive errors, respectively. The effect of ee is the dominant factor that appears during the evaporation period, while cc reflected the deviation in pyrolysis of blend oil rather than individual oils. The transition temperature which ee converted to cc were determined to be 460 °C as illustrated in Fig. 5 where the decomposition rates were similar and the traces were convened.

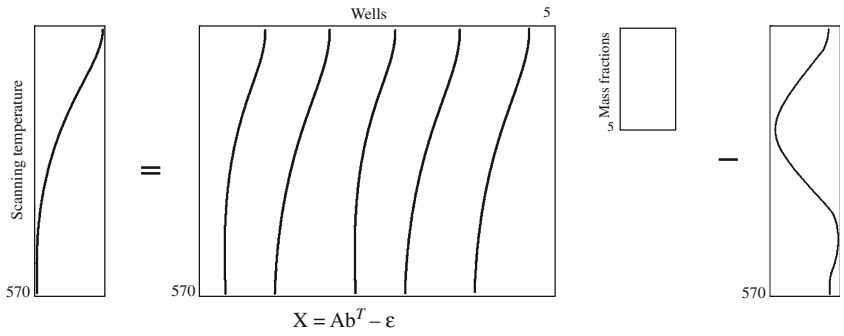

Fig. 6 Illustration of the principles of data that can be modeled with PLS method

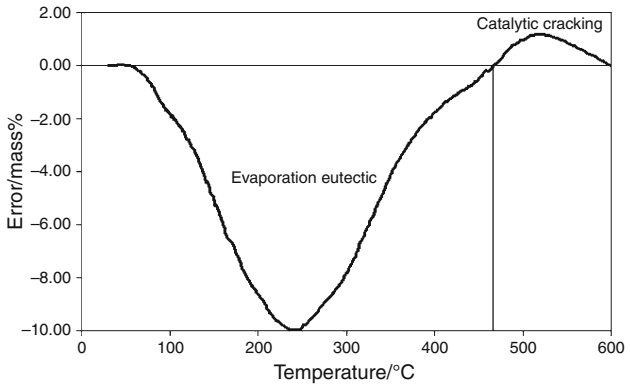

Fig. 7 The error diagram of normalized TG curve of blend oil

Conclusions

The pyrolysis behavior of oil samples from single wells and their blends was characterized using thermogravimetric traces to be used as fingerprints of each oil well sample. The thermal evaporation and degradation behavior of oil blends were correlated with that of the single well samples using partial least squares. It was shown that the WSM is appropriate for crude oil blends, which TG traces significantly differ from each other. However, if the pyrolysis curves have similar trends, it is difficult to distinguish between them. In the blend oil, the WSM gives larger errors due to the mixture reactions at higher temperatures than either of its components alone. Consequently, the fractions of single components are not correctly predicted even at low temperatures due to the changing the mass transfer coefficients and eutectic points. The proposed error function led to correct the blend equation by considering the eutectic points and catalytic pyrolysis in lower and higher temperatures, respectively. The proposed model has predicted the accurate oil wells productivity using a single sample point at the blend line.

Acknowledgements Financial support of the Shahreza Branch, Islamic Azad University (grant #51974891017001) is gratefully acknowledged. The authors wish to thank Mr. Sobhani for his prompt help in the laboratory of thermal analysis.

References

1. Thorn R, Johansen GA, Hammer EA. Recent developments in three-phase flow measurement. Meas Sci Technol. 1997;8:691–701.
2. Wang H, Priestman GH, Beck SBM, Boucher RF. A remote measuring flow meter for petroleum and other industrial applications. Meas Sci Technol. 1998;9:779–89.
3. Bostrom NW, Griffin DD, Kleinberg RL, Liang KK. Ultrasonic bubble point sensor for petroleum fluids in remote and hostile environments. Meas Sci Technol. 2005;16:2336–43.
4. Bernardie EB, Dubrunfaut O, Badot JC, Fourrier-Lamer A, Villard E, David PY, Jannier B, Grosjean N, Lance M. Low (10–800 MHz) and high (40 GHz) frequency probes applied to petroleum multiphase flow characterization. Meas Sci Technol. 2008;19:055602–8.
5. Tan C, Dong F. Modification to mass flow rate correlation in oil–water two-phase flow by a V-cone flow meter in consideration of the oil–water viscosity ratio. Meas Sci Technol. 2010;21:045403–14.
6. Wang J, Li F, Gardner RP. On the use of prompt gamma-ray neutron activation analysis for determining phase amounts in multiphase flow. Meas Sci Technol. 2008;19:094005–6.
7. Hilland J. Simple sensor system for measuring the dielectric properties of saline solutions. Meas Sci Technol. 1997;8:901–10.
8. Zhao B (2011) Numerical simulation for the temperature changing rule of the crude oil in a storage tank based on the wavelet finite element method. J Therm Anal Calorim. doi:10.1007/s10973-011-1469-x.
9. Kök MV (2010) Thermo-oxidative reactions of crude oils. J Therm Anal Calorim. doi:10.1007/s10973-010-1117-x.
10. Kök MV. Effect of pressure and particle size on the thermal cracking of light crude oils in sandstone matrix. J Therm Anal Calorim. 2009;97:403–7.
11. Streibel T, Geißler R, Saraji-Bozorgzad M, Sklorz M, Kaisersberger E, Denner T, Zimmermann R. Evolved gas analysis (EGA) in TG and DSC with single photon ionisation mass spectrometry (SPI-MS): molecular organic signatures from pyrolysis of soft and hard wood, coal, crude oil and ABS polymer. J Therm Anal Calorim. 2009;96:795–804.
12. Geißler R, Saraji-Bozorgzad M, Streibel T, Kaisersberger E, Denner T, Zimmermann R. Investigation of different crude oils applying thermal analysis/mass spectrometry with soft photoionisation. J Therm Anal Calorim. 2009;96:813–20.
13. Kök MV, Gundogar AS. Effect of different clay concentrations on crude oil combustion kinetics by thermogravimetry. J Therm Anal Calorim. 2010;99:779–83.
14. Streibel T, Fendt A, Geißler R, Kaisersberger E, Denner T, Zimmermann R. Thermal analysis/mass spectrometry using soft photo-ionisation for the investigation of biomass and mineral oils. J Therm Anal Calorim. 2009;97:615–9.

15. Kök MV. Influence of reservoir rock composition on the combustion kinetics of crude oil. J Therm Anal Calorim. 2009;97:397–401.
16. Fulem M, Becerra M, Hasan MDA, Zhao B, Shaw JM. Phase behaviour of Maya crude oil based on calorimetry and rheometry. Fluid Phase Equilib. 2008;272:32–41.
17. Gjurova KM, Ljubchev LA, Zagortcheva MK. Preliminary quantitative determination of petroleum and petroleum products in contaminated soils by using dynamic thermogravimetry. Thermochim Acta. 1999;335:55–61.
18. Shishkin YL. A new quick method of determining the group hydrocarbon composition of crude oils and oil heavy residues based on their oxidative distillation (cracking) as monitored by differential scanning calorimetry and thermogravimetry. Thermochim Acta. 2006;440:156–65.
19. Ferrasse JH, Chavez S, Arlabosse P, Dupuy N. Chemometrics as a tool for the analysis of evolved gas during the thermal treatment of sewage sludge using coupled TG–FTIR. Thermochim Acta. 2003;404:97–108.
20. Statheropoulos M, Mikedi K, Tzamtzis N, Pappa A. Application of factor analysis for resolving thermogravimetric–mass spectrometric analysis spectra. Anal Chim Acta. 2002;461:215–27.
21. Smidt E, Böhm K, Tintner J. Application of various statistical methods to evaluate thermo-analytical data of mechanically–biologically treated municipal solid waste. Thermochim Acta. 2010;501:91–7.
22. Miltyk W, Antonowicz E, Komsta L. Recognition of tablet content by chemometric processing of differential scanning calorimetry curves—an acetaminophen example. Thermochim Acta. 2010;507–508:146–9.
23. Serra R, Sempere J, Nomen R. A new method for the kinetic study of thermoanalytical data: the non-parametric kinetics method. Thermochim Acta. 1998;316:37–45.
24. Chrissafis K. Kinetics of thermal degradation of polymers: complementary use of isoconversional and model-fitting methods. J Therm Anal Calorim. 2009;95:273–83.
25. Kissinger HE. Reaction kinetics in differential thermal analysis. Anal Chem. 1957;29:1702–6.
26. Alvarez VA, Ruseckaite RA, Vazquez A. Kinetic analysis of thermal degradation in poly(ethylene–vinyl alcohol) copolymers. J App Poly Sci. 2003;90:3157–63.
27. Farjas J, Roura P. Modification of the Kolmogorov–Johnson–Mehl–Avrami rate equation for non-isothermal experiments and its analytical solution. Acta Mater. 2006;54:5573–9.
28. Avrami M. Kinetics of phase change. I General theory. J Chem Phys. 1939;7:1103–12.
29. Augis JA, Bennett JE. Calculation of the Avrami parameters for heterogeneous solid state reactions using a modification of the Kissinger method. J Therm Anal Calorim. 1978;13:283–92.
30. Ozawa T. A new method of analyzing thermogravimetric data. Bull Chem Soc Jpn. 1965;38:1881–6.
31. Perez-Maqueda LA, Sanchez-Jimenez PE, Criado JM. Kinetic analysis of solid-state reactions: precision of the activation energy calculated by integral methods. Int J Chem Kinet. 2005;37:658–66.
32. Horowitz HH, Metzger G. A new analysis of thermogravimetric traces. Anal Chem. 1963;35:1464–8.
33. Cozzani V, Petarca L, Tognotti L. Devolatilization and pyrolysis of refuse derived fuels: characterization and kinetic modelling by a thermogravimetric and calorimetric approach. Fuel. 1995;74:903–12.
34. Raveendran K, Ganesh A, Khilar KC. Pyrolysis characteristics of biomass and biomass components. Fuel. 1996;75:987–98.
35. Cozzani V, Stoppato G. A new method to determine the composition of biomass by thermogravimetric analysis. Can J Chem Eng. 1997;75:127–33.
36. Rajeswara RT, Sharma A. Pyrolysis rates of biomass materials. Energy. 1998;23:973–8.